

Heterogenised catalysts on zeolites. Synthesis of new chiral Rh(I) complexes with (2*S*,4*R*)-*trans*-4-RCOO-2-(*t*-butylaminocarbonyl)pyrrolidines and (2*S*,4*S*)-*cis*-4-RCONH-2-(*t*-butylaminocarbonyl)pyrrolidines. Heterogenisation on silica and a USY-zeolite and study of the role of support on their catalytic profile in hydrogenation of olefins

A. Corma^a, M. Iglesias^{b,*}, F. Mohino^b, F. Sánchez^c

^a Instituto de Tecnología Química, UPV-CSIC, Avda. de los Naranjos 46022 Valencia, Spain

^b Instituto de Ciencia de Materiales de Madrid, CSIC, Cantoblanco, 28049 Madrid, Spain

^c Instituto de Química Orgánica General, CSIC, Juan de la Cierva 3, 28006 Madrid, Spain

Received 22 January 1996; revised 14 May 1997

Abstract

Novel chiral ligands (2*S*,4*R*)-2-(*t*-butylaminocarbonyl)-4-[3-(alkylaminocarbonyl)propanoyloxy]pyrrolidine and (2*S*,4*S*)-*cis*-4-(alkylaminocarbonylamino)-2-(*t*-butylaminocarbonyl)pyrrolidine (**4a,b**; **9a,b**), (**a**: alkyl = *t*-butyl; **b**: alkyl = 3-triethoxysilylpropyl) and their rhodium complexes were synthesised and characterised. The reactions of $[\{\text{Rh}(\text{cod})\text{Cl}\}_2]$ and $[\text{RhCl}(\text{PPh}_3)_3]$ with the chiral ligands in the presence of a non-coordinating anion (PF_6^-) gave the cationic complexes $[\text{Rh}(\text{L}_2)(\text{ligand})][\text{PF}_6]$ ($\text{L}_2 = \text{cod}, \text{PPh}_3$). The structures of these complexes were elucidated by elemental analyses, IR spectroscopy and ^1H , ^{13}C and ^{31}P NMR measurements. The metal complexes bearing a triethoxysilyl group were covalently bonded to silica and modified USY-zeolite and Rh-heterogenised complexes were obtained. A comparative study (homogeneous versus supported) was made for the catalytic activity in hydrogenation reactions. © 1997 Elsevier Science S.A.

Keywords: Rhodium; Supported catalysts; Zeolites; Hydrogenation

1. Introduction

Rhodium, ruthenium and iridium complexes belong to the most developed class of homogeneous catalysts. Although many of these catalysts are highly active and selective in the hydrogenation of a large variety of unsaturated substrates, only few have been used on an industrial scale. Among others, one important technical problem is the separation and recovery of the soluble catalyst. Much effort has been made to solve this problem by anchoring such catalysts on a support [1]. Heterogenisation of selective homogeneous catalysts by use of insoluble supports in order to make their industrial application more economical remains a challenge [2–4].

However, in most cases immobilisation has caused severe reduction of the catalytic activity. Only a few investigations of the possible causes have been made. There are indications that besides the preparation method, other factors such as the pore size of insoluble supports or when working with organic polymer supports, the choice of solvents play a major role. Supported transition metal complexes attached to organic or inorganic supports have been widely investigated [5–7].

We have previously showed that rhodium complexes with very simple ligands derived from (*L*)-proline heterogenised on USY-zeolite are effective in the selective hydrogenation of various unsaturated substrates [8,9]. We found that the catalytic activity could be enhanced as a result of their immobilisation on supports. The main purpose of this work is the preparation of new series of chiral ligands based on *N,N'*-donor groups, starting from the easily available (*L*)-*trans*-4-hydroxy-

* Corresponding author. Tel.: +34-1-3349032; fax: +34-1-3720623; e-mail: immih3n@fresno.csic.es.

proline, synthesis of their Rh-complexes and the generation of their heterogenised silica and zeolite complexes. Finally, we have studied the effect of the ligands and the role of support on the catalytic profile of these complexes in the hydrogenation of olefins.

2. Experimental part

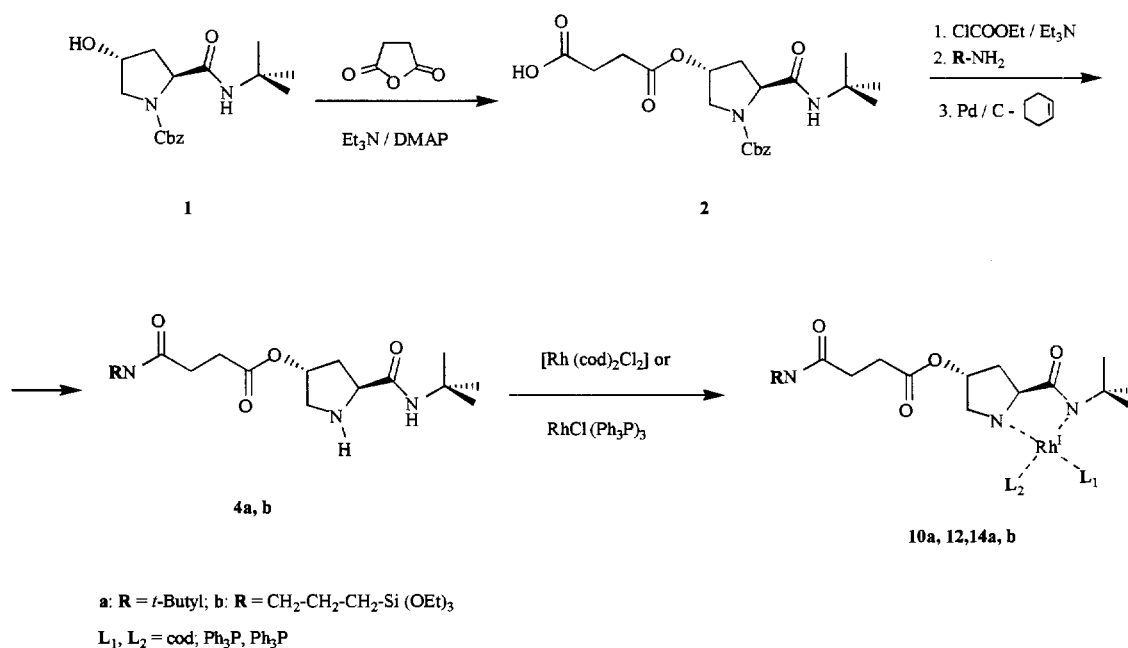
All preparations of organometallic complexes were carried out under dinitrogen by standard Schlenk techniques. The starting complexes $[\text{Rh}(\text{cod})\text{Cl}]_2$ and $[\text{RhCl}(\text{PPh}_3)_3]$ were prepared according to the literature methods [10–14]. All solvents were carefully degassed before use. The silylating agents $\text{OCN}(\text{CH}_2)_3\text{Si}(\text{OEt})_3$ and 3-aminopropyltriethoxysilane were obtained from Fluka (96% pure) and ABCR, respectively, and were distilled before use. C, H and N analysis were carried out by the analytical department of the Institute of Organic Chemistry and Institute of Materials Science (C.S.I.C.) with a Heraeus and a Perkin-Elmer 240C apparatus, respectively. Metal contents were analysed by atomic absorption using a Unicam Philips SP9 apparatus. The conductometric experiments were carried out in DMF (ca. 10^{-3} M) and acetonitrile (ca. 10^{-3} M) with a Pw5906 conductometer equipped with a Philips Pw 9510/60 conductometric cell. IR spectra were recorded with a Nicolet XR60 spectrophotometer (range $4000\text{--}200\text{ cm}^{-1}$) in KBr pellets; ^1H , ^{13}C and ^{31}P NMR spectra were taken on Varian XR300 and Bruker 200 spectrometers. ^1H NMR chemical shifts are given in

ppm using tetramethylsilane as an internal standard and ^{31}P NMR chemical shifts are downfield from 85% H_3PO_4 . Optical rotation values were measured at the sodium-D line (589 nm) with a Perkin Elmer 241 MC polarimeter. Gas chromatography analysis was performed using a Hewlett-Packard 5890 II with a flame ionisation detector in a cross-linked methylsilicone column.

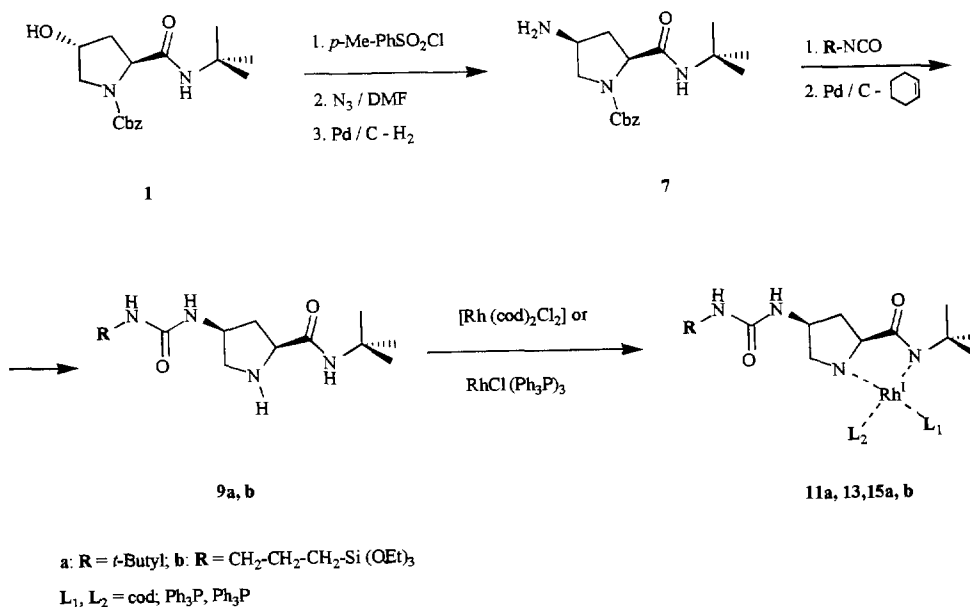
The inorganic supports taken as models were: SiO_2 Merck 60 (particle size 63–200 μm), and an ultrastable Y zeolite (USY) prepared by steam calcination at 1023 K of an 80% ammonium-exchanged NaY (SK40 Union Carbide), followed by treatment with a 1 N citric acid solution at 333 K for 30 min to remove extra-framework species. After this, the zeolite was thoroughly washed and dried at 403 K for 6 h. The final zeolite had a well-developed mesopores system (pore diameter 12–30 Å besides the typical ca. 12 Å micropores). The controlled dealumination promotes destruction of some sodalite units, which allowed direct communication between α -cages generating cavities wider than 12 Å. The formation of supermicropores and large mesopores has been detected by N_2 adsorption–desorption. The main characteristics of the resultant zeolite are: unit cell size: 24.40 Å, bulk $\text{SiO}_2/\text{Al}_2\text{O}_3$: 4.2, crystallinity: greater than 95%. The inorganic supports were dried at 415 K under 0.01 torr before the anchoring process.

2.1. Synthesis of ligands

Scheme 1 and Scheme 2 summarise the syntheses of the ligands. Complete experimental procedures, analyti-



Scheme 1. Preparation of the ligands **4a,b** and complexes.

Scheme 2. Preparation of the ligands **9a,b** and complexes.

cal and spectroscopic data are to be found as supplementary material deposited with the editor.

2.2. Synthesis of complexes

2.2.1. Synthesis of neutral complexes [RhCl(cod)(ligand)]

To a solution of di- μ -chloro-bis(1,5-cyclooctadiene)dirhodium (0.4 mmol) in dry dichloromethane (20 ml) was added a solution of the ligand (0.8 mmol) in dry dichloromethane (2 ml) and the mixture stirred for 3 h under room temperature under an argon atmosphere. The reaction mixture was filtered and the filtrate was evaporated under reduced pressure to 2 ml. Careful addition of diethyl ether caused the precipitation of a yellow–orange solid which was collected by filtration, washed with ethyl ether and/or pentane and dried in vacuo to give the desired complex.

2.2.1.1. [RhCl(cod)]{(2*S*,4*R*)-2-(*t*-butylaminocarbonyl)-4-[3-(*t*-butylaminocarbonyl)propanoyleoxy]pyrrolidine} (10a**). Yield: 82%. m.p. 97–98°C. $[\alpha]_{\text{D}}^{25} = -4.5$ ($c = 1.2$, EtOH). C₂₅H₄₃ClN₃O₄Rh (587.5): calc. C 51.1, H 7.4, N 7.2, Cl 6.1, Rh 17.5, found C 51.1, H 7.6, N 7.4, Cl 6.5, Rh 17.4. IR (cm⁻¹): $\nu = 3435, 3327, 3225\text{--}3216$ (N–H), 1737 (C=O_{ester}), 1658 (C=O_{amide}), 1602 (C=C), 330 (Rh–Cl). ¹H NMR (CDCl₃): $\delta = 5.2\text{--}5.1$ (m, 1H, CH–OCO), 4.3–4.1 (m, 4H, CH_{cod}), 4.0 (t, 1H, CH–NH), 3.3–3.1 (t, 2H, CH₂–NH), 2.6–2.5 (m, 2H, CH₂–CO₂), 2.5–2.3 (m, 6H, CH₂–CONH, 2 CH_{2cod}), 2.2–1.9 (m, 2H, CH₂–CH–OCO), 1.9–1.6 (m, 4H, 2 CH_{2cod}), 1.4 (s, 18H, CH₃). ¹³C NMR (DMSO): $\delta = 172.1$ (CONH–C(CH₃)₃), 170.9 (CH₂–CO₂), 170.0**

(CH₂–CONH), 81.6–81.2 (4 CH_{cod}), 74.2 (CH–OCO), 60.6 (CH–NH), 53.6 (C(CH₃)₃), 50.1 ((CH₃)₃C–NHCO–CH₂), 49.9 (CH₂–NH), 36.6 (CH₂–CH–OCO), 30.5 (CH₂–CO₂), 30.4 (2 CH_{2cod}), 29.2 (CH₂–CONH), 28.5 ((CH₃)₃C–NHCO–CH₂), 28.3 ((CH₃)₃C–NHCO–CH). UV–vis (CH₃CN, 10⁻³ M): λ_{max} (log ϵ) = 395 nm (3.63), 375 (3.88). A_{M} (Ω⁻¹ cm² mol⁻¹, 10⁻³ M): CH₃CN = 1.4, DMF = 1.4.

2.2.1.2. [RhCl(cod)]{(2*S*,4*S*)-2-(*t*-butylaminocarbonyl)-4-(*t*-butylaminocarbonylamino)pyrrolidine} (11a**). Yield: 57%. m.p. 135–136°C. $[\alpha]_{\text{D}}^{25} = -20.8$ ($c = 0.9$, EtOH). C₂₂H₄₀ClN₄O₂Rh (530.5): calc. C 49.8, H 7.5, N 10.5, Cl 6.7, Rh 19.4, found C 50.1, H 7.5, N 10.3, Cl 6.7, Rh 19.1. IR (cm⁻¹): $\nu = 3331$ (N–H), 1653 (C=O_{amide,urea}), 1600 (C=C), 330 (Rh–Cl). ¹H NMR (CDCl₃): $\delta = 4.3\text{--}4.2$ (m, 5H, CH–NH, 4 CH_{cod}), 4.2–4.0 (m, 1H, CH–NHCONH), 3.3–2.9 (m, 2H, CH₂–NH), 2.5–2.2 (m, 5H, CH_AH_B–CH–NHCONH, CH_{2cod}), 1.9–1.6 (m, 5H, 2 CH_{2cod}, CH_BH_A–CH–NHCONH), 1.4 (s, 9H, CH₃), 1.3 (s, 9H, CH₃). ¹³C NMR (CDCl₃): $\delta = 156.6$ (NHCONH), 77.6 (4 CH_{cod}), 62.6 (CH–NHCONH), 56.9 (CH₂–NH), 52.0 (CH–NH), 50.7 ((CH₃)₃C–NHCO–CH), 50.5 ((CH₃)₃C–NHCONH), 37.3 (CH₂–CH–NHCONH), 30.9 (CH_{2cod}), 29.6 ((CH₃)₃C–NHCONH), 28.7 ((CH₃)₃C–NHCOCH). UV–vis (CH₃CN, 10⁻³ M): λ_{max} (log ϵ) = 375 nm (3.80). A_{M} (Ω⁻¹ cm² mol⁻¹, 10⁻³ M): CH₃CN = 2.0.**

2.2.2. Synthesis of cationic complexes [Rh(cod)(N,N')][PF₆]

To a solution of di- μ -chloro-bis(1,5-cyclooctadiene)dirhodium (0.4 mmol) in dry dichloromethane (20

ml) was successively added a solution of the ligand (0.8 mmol) in dichloromethane (2 ml) and ammonium hexafluorophosphate (0.8 mmol). The mixture was stirred for 3 h at room temperature under argon atmosphere and filtered. The filtrate was evaporated under reduced pressure to 2 ml. Careful addition of diethyl ether caused the precipitation of a yellow–orange solid which was collected by filtration, washed with ethyl ether and dried in vacuo to give the desired cationic complex.

2.2.2.1. [Rh(COD)(2S,4R)-2-(*t*-butylaminocarbonyl)-4-[3-(*t*-butylaminocarbonyl)propanoyloxy]pyrrolidine]-[ClO₄]. (12a). Yield: 71%. m.p.: 146–148°C. [α]_D²⁵ = +20.7 (*c* = 1, EtOH). C₂₆H₄₅Cl₃N₃O₈Rh. (736.5): calc. C 42.4, H 6.1, N 5.7, Rh 14.0, found C 44.5, H 6.7, N 6.1, Rh 13.9. IR (cm⁻¹): ν = 3401, 3372, 3306 (N–H), 1737 (C=O_{ester}), 1655 (C=O_{amide}), 1604 (C=C), 1125 (Cl–O). ¹H NMR (CDCl₃): δ = 5.2 (s, 1H, CH–OCO), 4.6–4.4 (m, 1H, CH–NH), 4.4–4.3 (m, 2H, CH_A=CH_B)_{cod}, 4.2–4.0 (m, 2H, CH_B=CH_A)_{cod}, 3.4–3.1 (m, 2H, CH₂–NH), 2.9–2.2 (m, 10H, CH₂–CO₂, CH₂–CONH, 6 CH_{2cod}), 2.1–1.8 (m, 2H, CH₂–CH–OCO), 1.8–1.6 (m, 2H, CH₂)_{cod}, 1.4 (s, 9H, CH₃), 1.3 (s, 9H, CH₃). ¹³C NMR (CDCl₃): δ = 172.1 ((CH₃)₃C–NHCO–CH), 171.9 (CH₂–CO₂), 178 (CH₂–CONH), 79.3, 79.2, 79.1 y 78.9 (4 CH)_{cod}, 74.0 (CH–OCO), 64.0 (CH–NH), 54.9 (CH₂–NH), 54.1 ((CH₃)₃C–NHCO–CH), 51.3 ((CH₃)₃C–NHCO–CH₂), 37.0 (CH₂–CH–OCO), 31.8 (CH₂–CONH), 30.8 (2 CH₂)_{cod}, 30.3 (CH₂–CO₂), 28.7 ((CH₃)₃C–NHCO–CH₂), 28.2 (2 CH₂)_{cod}, 27.0 ((CH₃)₃C–NHCO–CH). UV–vis (CH₃CN, 10⁻³ M): λ_{max} . (log ϵ) = 370 (3.74). Λ_M (Ω⁻¹ cm² mol⁻¹, 10⁻³ M): CH₃CN = 11.5

2.2.2.2. Rh(cod)(2S,4R)-2-(*t*-butylaminocarbonyl)-4-[3-(3-triethoxysilylpropylaminocarbonyl)propanoyloxy]-pyrrolidine][PF₆]. (12b). Yield: 56%. m.p. 101–103°C. [α]_D²⁵ = +5.5 (*c* = 1, EtOH). C₃₀H₅₅F₆N₃O₇PRhSi (846): calc. C 42.6, H 6.6, N 5.0, Rh 12.2, found C 42.6, H 6.3, N 5.1, Rh 13.5. IR (cm⁻¹): ν = 3376, 3302, 3153 (N–H), 1741 (C=O_{ester}), 1656, 1652 (C=O_{amide}), 1603 (C=C), 844 (P–F). ¹H NMR (C₆D₆): δ = 4.8 (s, 1H, CH–OCO), 4.4–4.2 (m, 4H, CH_{cod}), 4.0–3.9 (m, 1H, CH–NH), 3.9–3.8 (q, 6H, O–CH₂–CH₃), 3.4–3.3 (m, 2H, CH₂–NHCO), 3.2–3.1 (m, 1H, CH_AH_B–NH), 2.9–2.8 (CH_BH_A–NH), 2.7–2.6 (m, 2H, CH₂–CO₂), 2.5–2.4 (m, 6H, CH₂–CONH, 2 CH_{2cod}), 2.3–2.2 (m, 1H, CH_AH_B–CH–OCO), 2.2–2.0 (m, 5H, CH_BH_A–CH–OCO, 2 CH_{2cod}), 1.9–1.7 (m, 2H, CH₂–CH₂–CH₂), 1.3 (t, 9H, O–CH₂–CH₃), 1.2 (s, 9H, CH₃), 0.7 (m, 2H, Si–CH₂). UV–vis (CH₃CN, 10⁻³ M): λ_{max} . (log ϵ) = 390 nm (3.69), 380 (3.90), 315 (3.87). Λ_M (Ω⁻¹ cm² mol⁻¹, 10⁻³ M): CH₃CN = 36.4, DMF = 12.3

2.2.2.3. [Rh(cod)(2S,4S)-2-(*t*-Butylaminocarbonyl)-4-(*t*-butylaminocarbonylamino)pyrrolidine][PF₆]. (13a). Yield: 77%. m.p.: 137–139°C. [α]_D²⁵ = +2.8 (*c* = 1, EtOH). C₂₃H₄₂Cl₂F₆N₄O₂PRh (725): C 38.1, H 5.8, N 7.7, Rh 14.2, found C 38.4, H 5.8, N 7.5, Rh 14.0. IR (cm⁻¹): ν = 3429, 3378, 3309 (N–H), 1660 (C=O_{amide,urea}), 1604 (C=C), 848 (P–F). ¹H NMR (CDCl₃): δ = 4.3–4.2 (m, 2H, 2 CH_{cod}), 4.2–4.0 (m, 4H, CH–NHCONH, CH–NH, CH_{cod}), 3.2–3.1 (m, 1H, CH_AH_B–NH), 2.7–2.6 (m, 1H, CH_BH_A–NH), 2.5–2.3 (m, 5H, CH_AH_B–CH–NHCONH, CH_{2cod}), 2.0–1.8 (m, 3H, CH_BH_A–CH–NHCONH, CH_{2cod}), 1.8–1.6 (m, 4H, CH_{2cod}), 1.3 (s, 18H, CH₃). UV–vis (CH₃CN, 10⁻³ M): λ_{max} . (log ϵ) = 375 nm (3.86), 310 (3.90). Λ_M (Ω⁻¹ cm² mol⁻¹, 10⁻³ M): CH₃CN = 42.2.

2.2.2.4. [Rh(cod)((2S,4S)-2-(*t*-Butylaminocarbonyl)-4-(3-triethoxysilylpropylaminocarbonylamino)-pyrrolidine-N,N')][PF₆]. (13b). Yield: 64%. m.p. 80–82°C. [α]_D²⁵ = +1.0 (*c* = 1, EtOH). C₂₇H₅₂F₆N₄O₅PRhSi (789): calc. C 41.1, H 6.6, N 7.1, Rh 13.0, found C 41.8, H 7.0, N 7.6, Rh 12.9. IR (cm⁻¹): ν = 3433, 3374, 3309 (N–H), 1658, 1651 (C=O_{amide, urea}), 1603 (C=C), 846 (P–F). ¹H NMR (C₆D₆): δ = 4.3–4.2 (m, 3H, CH–NHCONH, CH_{cod}), 4.3–4.1 (q, 6H, O–CH₂–CH₃), 4.2–4.1 (m, 2H, 2 CH_{cod}), 4.1–4.0 (m, 1H, CH–NH), 3.4–3.2 (m, 2H, CH₂–NHCONH), 3.1–2.9 (m, 1H, CH_AH_B–NH), 2.4–2.1 (m, 5H, CH_BH_A–NH, 2 CH_{2cod}), 2.3–2.1 (m, 1H, CH_AH_B–CH–NHCONH), 1.9–1.7 (m, 6H, 2 CH_{2cod}, CH₂–CH₂–CH₂), 1.8–1.7 (m, 5H, CH_BH_A–CH–NHCONH, 2 CH_{2cod}), 1.3 (m, 9H, CH₃), 1.2 (t, 9H, O–CH₂–CH₃), 0.7 (t, 2H, Si–CH₂). ¹³C NMR (C₆D₆): δ = 158.8 (NHCONH), 79.2, 79.1, 79.0, 78.9 (4 CH)_{cod}, 58.7 (O–CH₂–CH₃), 58.0 (CH–NH), 54.7 (CH–NHCONH), 53.4 (CH₂–NH), 51.1 ((CH₃)₃C–NHCO–CH), 43.5 (CH₂–NHCONH), 37.2 (CH₂–CH–NHCONH), 31.1, 28.5 (CH₂)_{cod}, 28.4 ((CH₃)₃C–NHCONH), 24.2 (CH₂–CH₂–CH₂), 18.6 (O–CH₂–CH₃), 8.3 (Si–CH₂). UV–vis (CH₃CN, 10⁻³ M): λ_{max} . (log ϵ) = 380 nm (3.89), 315 nm (3.88). Λ_M (Ω⁻¹ cm² mol⁻¹, 10⁻³ M): CH₃CN = 34.0, DMF = 19.8

2.2.3. General procedure for synthesis of Wilkinson-type derivatives [Rh(L)(PPh₃)₂][PF₆]

To a solution of [RhCl(PPh₃)₃] (0.2 mmol) in dry dichloromethane (20 ml) the stoichiometric amount of the corresponding ligand in dichloromethane (2 ml) and NH₄[PF₆] were added. The mixture was heated under reflux for 3–5 h under argon atmosphere and the NH₄Cl filtered off. The filtrate was evaporated to 5 ml, diethyl ether was carefully added with stirring and the yellow–orange powder thus formed was collected, washed with ethyl ether and dried in vacuo.

2.2.3.1. $[Rh(PPh_3)_2]\{(2S,4R)\text{-}2\text{-}(t\text{-butylaminocarbonyl})\text{-}4\text{-}[3\text{-}(t\text{-butylaminocarbonyl})\text{propanoyloxy}]\text{pyrrolidine}\}\text{-}[PF_6]$ (**14a**). Yield: 79%. m.p. 133–135°C. $[\alpha]_D^{25} = -80.3$ ($c = 1$, EtOH). $C_{54}H_{63}Cl_2F_6N_3O_4P_3Rh$ (1198): calc. C 54.1, H 5.3, N 3.5, Rh 8.6, found C 54.1, H 5.4, N 3.6, Rh 8.8. IR (cm^{-1}): $\nu = 3414, 3364, 3297$ (N–H), 1737 (C=O_{ester}), 1653 (C=O_{amide}), 842 (P–F). 1H NMR ($CDCl_3$): $\delta = 7.7\text{--}7.0$ (m, 30H, Ph), 5.3–5.2 (m, 1H, CH–OCO), 4.3–4.2 (m, 1H, CH–NH), 3.8–3.7 (m, 1H, CH_AH_B–NH), 3.6–3.5 (m, 1H, CH_BH_A–NH), 2.6–2.5 (m, 3H, CH₂–CO₂, CH_AH_B–CH–OCO), 2.5–2.3 (m, 2H, CH₂–CONH), 2.2–2.1 (m, 1H, CH_BH_A–CH–OCO), 1.3 (s, 9H, CH₃), 1.0 (s, 9H, CH₃). ^{31}P NMR ($CDCl_3$): $\delta = 41.4$ (PPh₃); -143.6 (PF₆). UV–vis ($CH_3CN, 10^{-3}$ M) λ_{max} (log ϵ): 405 nm (3.77), 330 (4.15). Λ_M ($\Omega^{-1} cm^2 mol^{-1}, 10^{-3}$ M): $CH_3CN = 48.1$.

2.2.3.2. $[Rh(PPh_3)_2]\{(2S,4R)\text{-}2\text{-}(t\text{-butylaminocarbonyl})\text{-}4\text{-}[3\text{-}(3\text{-triethoxysilylpropylaminocarbonyl})\text{propanoyloxy}]\text{pyrrolidine}\}\text{-}[PF_6]$ (**14b**). Yield: 58%. m.p. 169–171°C. $C_{60}H_{75}Cl_2F_6N_3O_7P_3RhSi$ (1347): calc. C 52.6, H 5.6, N 3.1, Rh 7.6, found C 52.1, H 5.6, N 3.6, Rh 7.3. IR (KBr): $\nu = 3362, 3295, 3142$ (N–H), 1739 (C=O_{ester}), 1653 (C=O_{amide}), 843 (P–F). 1H NMR (C_6D_6): $\delta = 8.0\text{--}6.8$ (m, 30H, Ph), 5.4–5.3 (m, 1H, CH–OCO), 4.9–4.8 (m, 1H, CH–NH), 3.9–3.8 (m, 1H, CH_AH_B–NH), 3.9–3.8 (q, 6H, O–CH₂–CH₃), 3.7–3.6 (m, 1H, CH_BH_A–NH), 3.2–3.1 (m, 2H, CH₂–NHCO), 3.2–2.2 (m, 1H, CH_AH_B–CH–OCO), 2.8–2.7 (m, 1H, CH_BH_A–CH–OCO), 2.6–2.5 (m, 2H, CH₂–CO₂), 2.4–2.3 (m, 2H, CH₂–CONH), 1.7–1.6 (m, 2H, CH₂–CH₂–CH₂), 1.3 (t, 9H, O–CH₂–CH₃), 1.0 (s, 9H, CH₃), 0.7–0.6 (m, 2H, Si–CH₂). ^{31}P NMR ($CDCl_3$): $\delta = 40.8$ (PPh₃); -143.8 (PF₆). UV–vis ($CH_3CN, 10^{-3}$ M) λ_{max} (log ϵ): 400 nm (3.72), 385 (3.82), 330 (4.12), 320 (4.13). Λ_M ($\Omega^{-1} cm^2 mol^{-1}, 10^{-3}$ M): $CH_3CN = 50.8$.

2.2.3.3. $[Rh(PPh_3)_2]\{(2S,4S)\text{-}2\text{-}(t\text{-Butylaminocarbonyl})\text{-}4\text{-}(t\text{-butylaminocarbonylamino})\text{pyrrolidine}\}\text{-}[PF_6]$ (**15a**). Yield: 60%. m.p. 140–142°C. $[\alpha]_D^{25} = -57.8$ ($c = 1$, EtOH). $C_{51}H_{60}Cl_2F_6N_4O_2P_3Rh$ (1141): calc. C 53.6, H 5.3, N 4.9, Rh 9.0, found C 53.0, H 5.4, N 4.6, Rh 9.2. IR (cm^{-1}): $\nu = 3420, 3361, 3297$ (N–H), 1669, 1653 (C=O_{amide.urea}), 842 (P–F). 1H NMR ($CDCl_3$): $\delta = 7.7\text{--}7.1$ (m, 30H, Ph), 3.7–3.6 (m, 1H, CH–NHCONH), 4.2–4.1 (m, 1H, CH–NH), 2.7–2.5 (m, 2H, CH_AH_B–NH, CH_AH_B–CH–NHCONH), 2.5–2.4 (m, 1H, CH_BH_A–NH), 2.3–2.1 (m, 2H, CH_BH_A–NH, CH_BH_A–CH–NHCONH), 1.3 (s, 9H, CH₃), 1.0 (s, 9H, CH₃). UV–vis ($CH_3CN, 10^{-3}$ M): λ_{max} (log ϵ) = 405 nm (3.78), 345 (4.08), 325 (4.07). Λ_M ($\Omega^{-1} cm^2 mol^{-1}, 10^{-3}$ M): $CH_3CN = 42.4$.

2.2.3.4. $[Rh(PPh_3)_2]\{(2S,4S)\text{-}2\text{-}(t\text{-Butylaminocarbonyl})\text{-}4\text{-}(3\text{-triethoxysilylpropylaminocarbonylamino})\text{pyrrolidine}\}\text{-}[PF_6]$ (**15b**). Yield: 72%. m.p. 113–115°C. $[\alpha]_D^{25} = -15.9$ ($c = 1$, EtOH). $C_{58}H_{72}Cl_2F_6N_4O_5P_3RhSi$ (1302): calc. C 52.1, H 5.6, N, 4.3, Rh 8.0, found C 51.6, H 5.8, N 4.7, Rh 7.7. IR (cm^{-1}): $\nu = 3420, 3361, 3297$ (N–H), 1653 (C=O_{amide.urea}), 842 (P–F). 1H NMR (C_6D_6): $\delta = 7.8\text{--}6.9$ (m, 30H, Ph), 4.7–4.6 (m, 1H, CH–NHCONH), 4.1–4.0 (m, 1H, CH–NH), 3.9–3.8 (q, 6H, O–CH₂–CH₃), 3.2–3.0 (m, 2H, CH₂–NHCONH), 3.1–2.9 (m, 1H, CH_AH_B–NH), 2.8–2.7 (m, 1H, CH_BH_A–NH), 2.3–2.2 (m, 1H, CH_AH_B–CH–NHCONH), 1.8–1.7 (m, 1H, CH_BH_A–CH–NHCONH), 1.7–1.5 (m, 2H, CH₂–CH₂–CH₂), 1.2 (t, 9H, O–CH₂–CH₃), 1.1 (s, 9H, CH₃), 0.7 (t, 2H, Si–CH₂). UV–vis ($CH_3CN, 10^{-3}$ M): λ_{max} (log ϵ) = 410 nm (3.71), 325 (4.04), 300 (4.03). Λ_M ($\Omega^{-1} cm^2 mol^{-1}, 10^{-3}$ M): $CH_3CN = 50.1$, DMF = 1.6.

2.3. Anchoring of complexes

A dry toluene suspension (40 ml) of an inorganic support (silica or modified USY-zeolite pre-dried at 140°C for 3–4 h in vacuo) (1 g) was stirred under argon for 2 h at room temperature. A rhodium complex of **10b–15b** bearing a triethoxysilyl group, (0.2 meq.) in dry dichloromethane (2 ml) was then dropwise added and the mixture stirred for 24 h under argon at room temperature. The solid was then filtered and Soxhlet-extracted with dichloromethane/ethyl ether (1:2) for 7–12 h in order to remove the remaining non-bonding complex and dried in vacuo. Analytical data for the heterogenised Rh-complexes are given in Table 1.

2.4. Catalytic experiments

The catalytic properties of the above homogeneous and heterogenised Rh-complexes were examined under conventional conditions for batch reactions in a reactor (Autoclave Engineers) of 100 ml capacity at tempera-

Table 1
Analytical data for heterogenised complexes

| Comp. | Analysis found (calc.) | | | | Anchoring (%) |
|-----------------|------------------------|-----------|-----------|-----------|---------------|
| | %C | %H | %N | %Rh | |
| Sil-12b | 5.9 (6.0) | 1.4 (0.8) | 0.8 (0.9) | 0.9 (1.1) | 95 |
| Zeol-12b | 3.3 (3.0) | 0.5 (0.4) | 0.5 (0.4) | 0.6 (0.8) | 63 |
| Sil-13b | 3.8 (3.8) | 0.7 (0.6) | 0.9 (0.7) | 0.8 (0.8) | 88 |
| Zeol-13b | 3.1 (2.8) | 1.0 (0.5) | 0.5 (0.5) | 0.8 (1.1) | 79 |
| Sil-14b | 5.4 (5.8) | 0.5 (0.7) | 0.5 (0.5) | 0.9 (1.0) | 68 |
| Zeol-14b | 5.0 (3.0) | 2.0 (0.3) | 0.4 (0.2) | 0.6 (0.4) | 36 |
| Sil-15b | 5.8 (5.1) | 2.0 (1.6) | 0.7 (0.4) | 0.7 (1.0) | 70 |
| Zeol-15b | 5.1 (5.6) | 2.0 (2.3) | 0.6 (0.9) | 0.6 (1.1) | 45 |

Table 2

Turnover numbers (mmol substrate/mmol cat. s) in the maximum rate for the hydrogenation of hex-1-ene, cyclohexene and methyl cyclohexene ^a

| Catalyst | hex-1-ene ^b | cyclohexene ^b | methylcyclohexene | $\frac{U_{\max}^{\text{hex-1-ene}}}{U_{\max}^{\text{cyclohexene}}}$ |
|-------------------------|------------------------|--------------------------|-------------------|---|
| 12a ^c | 221(6) | 76(10) | 1.5 | 2.9 |
| Sil-12b | 113 | 44 | 1.4 | 2.0 |
| Zeol-12b | 307 | 137 | 7 | 3.0 |
| 13a ^c | 87.2 | 52.5 ^c | 5.2 | 1.6 |
| Sil-13b | 459.8 | 248.1 | 0.6 | 1.8 |
| Zeol-13b | 434.7 | 213.5 | 0.7 | 2.0 |

^a Cat./subs.: 1/10,000; $T = 323$ K, $P_{\text{H}_2} = 6$ atm.

^b induction time (min.) in parenthesis;

^c decomposition of catalyst (Rh(0) particles)

tures, dihydrogen pressures and Rh/substrate molar ratios indicate in each reaction type.

2.4.1. Hydrogenation of simple olefins

Hex-1-ene, cyclohexene and 1-methylcyclohexene (high purity Merck) were hydrogenated in a batch reactor at 335 K reaction temperature, 5 atm of dihydrogen pressure, and Rh/substrate molar ratio 1/100000 for 1-hexene and cyclohexene, and 1/10000 for 1-methyl cyclohexene. In a standard experiment the olefin was added to a solution (homogeneous catalysts) or suspension (heterogenised catalysts) of catalytic material in methyl *iso*-butylketone (50 ml) and the mixture was stirred under dihydrogen pressure. The evolution of the reaction was monitored by g.l.c. on a capillary silicone column using nitrogen as carrier (see Table 2). After hydrogenation, the homogeneous catalysts was removed by filtration through a short celite column, whilst the heterogenised supported was separated by simple filtration and used again.

2.4.2. Hydrogenation of prochiral olefins

In a typical experiment ethyl (Z)- α -acetylaminocinnamate, selected as a model compound, was hydrogenated in a batch reactor at 338 K, 5 atm of dihydrogen pressure and a catalyst/substrate molar ratio 1/100. The olefin (2 mmol) was added to a solution (homogeneous catalysts) or suspension (heterogenised catalysts) of the catalytic material in ethanol (45 ml) and the reactor was purged with nitrogen. The reaction mixture was heated to 338 K, pressurised with dihydrogen and stirred. The reaction was monitored by HPLC on a C18

Table 3

Recycling of catalyst **Zeol-13b** in hydrogenation of cyclohexene

| Run | Time (conversion at 10 min) | Tor (mmol/mmolcat.s) |
|----------|-----------------------------|----------------------|
| 1 | 63.4 | 104 |
| 2 | 68.6 | 133 |
| 3 | 81.3 | 225 |
| 4 | 63.9 | 117 |

Table 4

Asymmetric hydrogenation of Z(α)-ethyl acetamidocinnamate and Z(α)-ethyl benzamidocinnamate (cat./subs. = 1/100, $T = 60^\circ\text{C}$; $P_{\text{H}_2} = 5$ atm)

| Catalyst | Z-(α)-ethyl acetamidocinnamate | | Z-(α)-ethyl benzamidocinnamate | |
|-----------------|---|--------------------|---|--------------------|
| | TOR ^a | ee(%) ^b | TOR ^a | ee(%) ^b |
| 12a | 32.3 | 88.7 | 13.1 | 91.6 |
| Sil-12b | 26.7 | 76.1 | 16.2 | 87.6 |
| Zeol-12b | 20.3 | 55.1 | 6.9 | 84.1 |
| 13a | 15.2 | 34.5 | 16.3 | 57.4 |
| Sil-13b | 12.6 | 29.9 | 22.5 | 54.3 |
| Zeol-13b | 12.6 | 46.9 | 22.5 | 62.3 |

^a mmol substrate/mmol cat. s;

^b S configuration.

reversed phase using methanol: water (1/1.1) as eluent with UV detection at 228 nm (see Table 4). After hydrogenation, the homogeneous catalysts was removed by filtration through a short column of celite, whilst the heterogenised supported was separated by simple filtration and used in a new run.

3. Results and discussion

3.1. Ligand synthesis

The synthesis of (2*S*,4*R*)-*trans*-2-(*t*-butylamino-carbonyl)-4-[3-(alkylaminocarbonyl)propanoyleoxy]pyrrolidine (**4a,b**) is outlined in Scheme 1 and was used to prepare the homogeneous catalyst. The *t*-butyl group was replaced by a 3-triethoxysilylpropyl group to prepare heterogenised catalysts. All reaction steps were tuned for high yield and selectivity, taking special care to exclude any hydrolysis-polymerisation of triethoxysilyl groups. Thus, starting from the easily available (2*S*,4*R*)-*trans*-4-hydroxyproline it was quantitatively protected as the *N*-carbobenzyloxy derivative by treatment with benzyl chloroformate and sodium hydroxide. This *N*-protected aminoacid was converted into the corresponding *t*-butylamide **1**, by a quantitative two-step reaction, treatment with ethyl chloroformate and triethylamine obtaining a mixed anhydride and reaction with *t*-butylamine. The hydroxyamide **1** was selectively *O*-acylated by succinic anhydride in presence of a molar amount of triethylamine and 10% of dimethylaminopyridine as catalysts to give the succinic hemiester **2**. The hemiester **2** was converted in its corresponding amide-ester **3** by reaction of the carboxylic group with *t*-butylamine (**a**) or 3-triethoxysilylpropylamine (**b**), *via* mixed-anhydride, to yield **3a,b**. The ligands **4a,b** were made by hydrogenolytic cleavage of the *N*-carbobenzyloxy groups using 10% Pd/C as catalysts and cyclohexene as hydrogen source in refluxing ethanol.

The synthesis of (2*S*,4*S*)-*cis*-4-alkylaminocarbonylamino-2-*t*-butylaminocarbonylpyrrolidine (**9a,b**) was started from (2*S*,4*R*)-1-benzyloxycarbonyl-2-*t*-butylaminocarbonyl-4-hydroxypyrrolidine (**1**), synthesised as above, as shown in Scheme 2. Thus, the amide **1** was quantitatively *O*-tosylated with *p*-toluenesulphonylchloride in toluene, the resulting 4-tosyl group was replaced by an azido group stereospecifically with inversion of the configuration at C-4 to yield (2*S*,4*S*)-4-azido-1-benzyloxycarbonyl-2-*t*-butylaminocarbonylpyrrolidine (**6**). In compound **6**, the 4-azido group was selectively reduced in presence of 10% Pd/C with hydrogen at 1 atm in ethyl acetate for 16 hours to yield amine **7** (97%). Under the conditions used the *N*-benzyloxycarbonyl group remains intact, protecting the secondary amine in the subsequent reactions. The primary amine **7** reacts with *t*-butylisocyanate or 3-triethoxysilylpropylisocyanate to affords the urea **8a,b**, respectively. In the last step the *N*-protecting group was cleaved using Pd/C as catalyst and cyclohexene as hydrogen source in refluxed ethanol yielding **9a,b**.

All intermediates and N,N'-donors has been obtained with a total yield of 77–90% and were characterised unequivocally by, mass, IR and ¹H and ¹³C NMR spectra and gave satisfactory elemental analyse.

3.2. Synthesis and characterisation of Rh-complexes

Addition of a stoichiometric amount of donor (**4a,b** and **9a,b**) to a dichloromethane solution of complex precursor [$\{\text{RhCl}(\text{cod})\}_2$] leads to the formation of neutral complexes $[\text{RhCl}(\text{cod})(\text{ligand})]$ (**10a,b**, **11a,b**) by cleavage of the chloride bridge mediated by nucleophilic attack of N,N'-donor. The complexes were isolated as yellow, relatively air-stable solids that present a well defined Rh–Cl band in their IR spectra. When the same reaction was carried out in the presence of a non-coordinating anion, such as, ammonium hexafluorophosphate, complex formation and the replacement of the chloride ion take place simultaneously yielding the corresponding cationic complexes $[\text{Rh}(\text{cod})(\text{ligand})][\text{PF}_6]$ (**13a,b**, **14a,b**). The complexes were isolated as orange–yellow air-stable solids. Microanalytical, conductivity and IR spectroscopic data are given in Section 2. The analogous PPh₃ complexes **14a**, **15a** can be conveniently obtained following the same procedure starting from $[\text{RhCl}(\text{PPh}_3)_3]$ and **4a**, they were isolated as yellow, air-stable solids. Some precautions, i.e., low temperatures and the exclusion of water and hydroxylic solvents, have to be taken only in the case of aminopropyltriethoxysilane derivatives, to avoid hydrolysis and subsequent polymerisation. Since no suitable crystals could be obtained, the structures of the complexes were determined by IR and NMR spectroscopy, and elemental analyse.

The spectroscopic data and the elemental analyse are

in agreement with the bidentate proposed structures. Thus, the IR spectra show the presence of the coordinated diene and bands for the co-ordinated N,N-donors slightly shifted respect to the free ligands. The spectra show $\nu(\text{N–H})$ at higher frequencies than in the free donors which indicates Rh–N co-ordination; the values for the C=O amide are close to the values of the free base and excludes linkage of the ligand through the C=O group (Rh–O bond) but the $\nu(\text{C=O})$ ester appears at higher frequencies than the free ligands ($+24 \text{ cm}^{-1}$) which indicates that exists some Rh–O interaction. A defined band at $350\text{--}360 \text{ cm}^{-1}$ corresponding to $\nu(\text{RhCl})$ appears in neutral complexes and an additional band at $\sim 845 \text{ cm}^{-1}$ due to $\nu(\text{P–F})$ in cationic complexes. Bands corresponding to phosphine, cod and *t*-butyl groups appear at their expected frequencies.

The ¹H and ¹³C NMR spectra show the signals corresponding to ring protons and carbons slightly downfield shifted with respect to the free bases, and signals of the atoms close to the metal are remarkably broadened due to the metal interactions and to conformational non-rigidity on the NMR time scale. On the other hand, the cyclooctadiene and triphenylphosphine ligands give rise to resonances in the expected positions [16,17].

Electronic absorption spectra of the rhodium-complexes generally show two or three absorption bands in the 400–300 nm region. The two bands at 400 nm with $\epsilon = 10^3\text{--}10^4$ may be assigned to the Rh → ligand (chiral ligand, PPh₃) and Rh → cod charge transfer transition and highest energy band around 300 nm with $\epsilon = 10^3\text{--}10^4$ corresponds to an intra-ligand transition, both values are close to wavelengths and extinction coefficients published for related complexes.

The conductivity data suggest 1:1 electrolytes for cationic complexes **13–15a,b** [18,19].

3.3. Heterogenisation of Rh-complexes

The treatment of inorganic oxides with metal complexes containing an anchor group is a common way to generate supported catalysts as we have previously reported [4,15]. Ligands in complexes of this type consist of a 'sticky-end' ($-\text{Si}(\text{OEt})_3$, $-\text{SiX}_3$) which can be linked to the support surface via a mono or bidentate ligand group and a spacer, mainly, $(-\text{CH}_2-)_n$, which connect these two functional units. Following this methodology, that assures a uniform distribution on the support surface and well characterised structures for the Rh-complexes analysed before anchoring by conventional methods, preparations of heterogenised complexes were carried out for complexes **10b–15b**, bearing a $-\text{CH}_2\text{CH}_2\text{CH}_2\text{Si}(\text{OEt})_3$ group, by controlled hydrolysis of Si–OEt bonds and reaction with the free silanol (Si–OH) on the surface of the silica or an USY-zeolite. The resulting catalytic material are very

stable and the species are covalently bonded to the surface. To confirm that all materials were covalently bonded the crude solids were thoroughly Soxhlet-extracted with methylene chloride-ethyl ether for 12 hours to remove unbound metal complexes and then were dried in high vacuum. The percentage of complex of the new materials was obtained by elemental analysis of C,H,N and the contents of the metal was determined by atomic absorption of Rh, the results were shown in Table 1. These values ($\sim 1\%$) have been used for calculating the ratio catalyst/substrate in the reaction tests.

These heterogenised complexes are characterised by IR, UV-vis and elemental analysis of C, H, N and Rh. The fact that the structures of the starting complexes are maintained when attached to the surface was confirmed by spectroscopic data. It is unlikely that the nature of the complex is substantially altered under the relatively mild conditions of the anchoring reaction [20]. The anchoring process was performed by treatment of the solid in a solution of complex in toluene at room temperature for 24 h. The loading of the metal is always ca. 1% ($\pm 0.1\%$), measured by atomic absorption of rhodium of the digested samples. In several preparations the sequences ligand \rightarrow complex \rightarrow anchoring were altered without significant change in the quality of the supported catalysts obtained.

Several supports were selected: silica that is a popular support, since it is resistant against elevated temperatures and most solvents and its surface properties are already well defined [21] and a modified zeolite that exhibits some exceptional properties different from those containing simple oxide-bound ones. Such modifications may result from 'the molecular sieve' properties of the zeolite microcrystals, it promotes a concentration effects for the reagents on the surface and added the possibility that three dimensional steric constraints into the microporosity or supercage cavities of support where the reaction takes place and could influence on the

substrate-catalyst interaction [22]. Of particular interest to us is the possibility that the cage environment has effects on the reactivity of substrate molecules and selectivity of reactions through specific substrate/environment interactions.

3.4. Reactivity

3.4.1. Catalytic hydrogenation of simple olefins

Hex-1-ene, cyclohexene and 1-methylcyclohexene were hydrogenated in the presence of soluble catalysts and the corresponding silica and zeolite heterogenised complexes. In all experiments with *soluble* catalysts we observed an induction period which extended, depending on the catalyst employed, from 5 min to 10 min for 1-hexene and cyclohexene and higher for methyl cyclohexene, and in this initial time of the reaction, presence of the isomerisation products (up to 20% conversion) for 1-hexene were detected. The induction period disappears in case of heterogenised catalysts on zeolite and isomerisation could not be detected.

The maximum rate of hydrogenation of the three olefins was shown to be in the order: hex-1-ene > cyclohexene \gg 1-methylcyclohexene. Thus, for hex-1-ene reduction, the cationic complexes supported on zeolite **Zeol-12b**, **13b** are more active than when supported on silica or when unsupported (Fig. 1). Therefore, it seems that the enhanced surface concentration effect and/or an electrical interaction between the substrate and the zeolite support could indeed be responsible for both the absence of an induction effect and its higher activity. The turnover numbers for a series of catalysts are given in Table 2. It can be seen that hex-1-ene is indeed hydrogenated more quickly than cyclohexene on the homogeneous catalyst, and for 1-methylcyclohexene maximum rates are similar for all catalysts studied. Moreover the order of activity for cyclohexene also follows the order: zeolite > homogeneous > silica. The kinetic curves are shown in

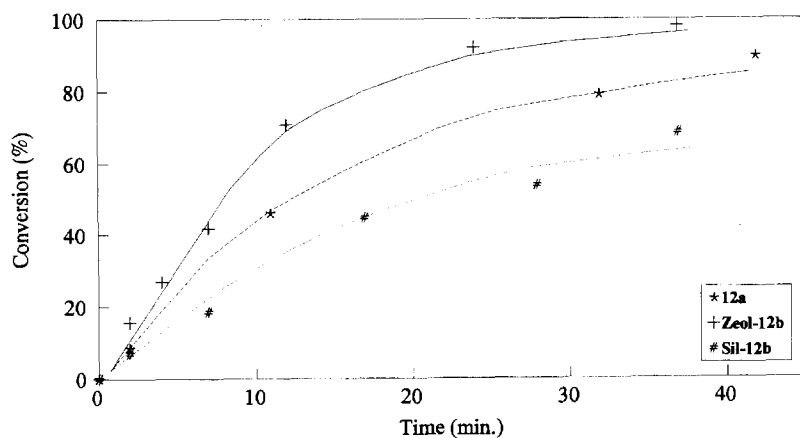


Fig. 1. Hydrogenation of cyclohexene with cationic catalysts (**12a**, **Sil-12b**, **Zeol-12b**).

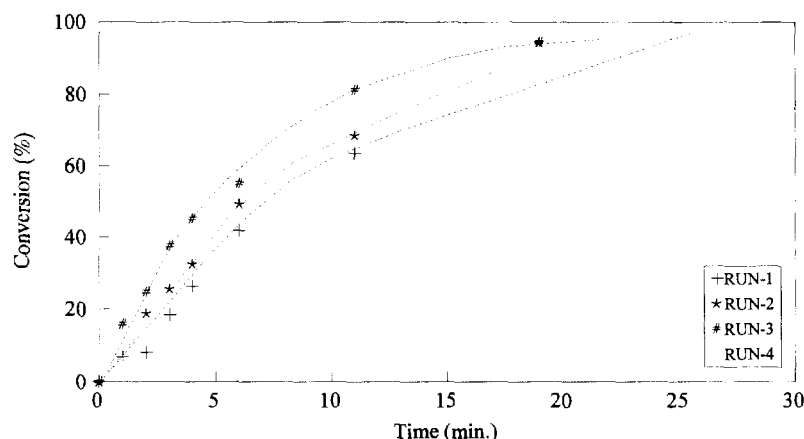


Fig. 2. Recycling of catalyst Zeol-13b.

Fig. 1. The activity of the cationic complexes did not decrease after several runs (Fig. 2, Table 3).

Nevertheless, as shown in Table 2, the hexene/cyclohexene hydrogenation ratio is lower for the homogeneous catalyst than for the zeolite-supported catalyst. This result may indicate that in general geometrical constraints for bulkier molecules follow the expected order: zeolite > silica, homogeneous.

In conclusion, for hex-1-ene and cyclohexene, when cationic complexes were supported on a neutral carrier such as silica, a decrease in maximum rates was found with respect to the homogeneous one. These results agree with those previously reported on the effect of supporting complexes on solid carriers. In contrast, the results observed when using a USY-zeolite as support indicated that there is no detectable induction period, and the maximum rates increase dramatically. Since the main differences between the silica and USY-zeolite are the presence of strong electric fields and cavities in the latter, we believe that the observed phenomena could be related to both a concentration effect and charge interactions with the surface. It must be pointed out that one cannot expect the whole zeolite to participate in this process, but mainly the most external open cavities, which form supermicropores and contain the anchored complexes. The supermicropores and mesopores are formed during steam dealumination [23].

On the other hand, the introduction of a methyl group attached to a double bond when using 1-methylcyclohexene causes a decrease in the hydrogenation rate, even for the homogeneous catalyst. Moreover, this decrease is much higher in the case of the zeolite-supported one; similar rates are observed for all catalysts, supported and unsupported. This fact indicates that when geometrical constraints for the coordination of the olefin to the metal become more important, the geometrical limitations due to the carrier become secondary.

Amongst the *soluble* catalysts the phosphine derivatives were found to have the highest activity but their

composition changes with the reaction evolution and the maximum rates correspond to the initial rates and decreasing later. Anchoring these type of complexes to a silica and zeolite supports produces an increase in activity in the first operation but activity is decreased in the subsequent runs.

Moreover, in the homogeneous reactions, the colour darkened gradually, and sometimes brown or black particles of Rh(0) separated towards the end of processes and the soluble complexes could be used only once. If more olefin was added after the reaction was completed, no hydrogenation occurred. The heterogenised complexes on silica- or zeolite-complexes became more stable, could be recovered by simple filtration and recycling in further runs without loss of activity. This behaviour have been demonstrated since in the IR spectra of recovered heterogenised catalyst could be detected bands at 2040–2100 cm^{-1} that suggests the existence of stable Rh(III) hydrides anchored on the surface which must be responsible for hydrogenation activity.

3.4.2. Hydrogenation of dehydroaminoacid derivatives

The Rh-catalysts were also tested for enantioselective hydrogenation of ethyl (*Z*)- α -acetamido- and α -benzamido-cinnamates (1/100 catalyst/substrate ratio) in mild conditions yielding the corresponding phenylalanine derivatives with quantitative conversion and moderate enantioselectivity (Table 4). For the two substrates tested and using the same amount of rhodium, when homogeneous cationic- or silica-heterogenised complexes were used, a remarked induction period was observed (wider than the observed for simple olefins) due to the slow formation of catalytic active species, on the contrary when cationic complexes were supported on an modified USY-zeolite no induction period was detected as a consequence of the known strong capability of zeolites to adsorb H_2 on surface that increases the local concentration of hydrogen. An-

other feature to be remarked is that, when transition metal complexes have been supported on carrier such as polymers or silica, etc., a strong reduction in the reactivity has been observed. However, in our case the turnover numbers for hydrogenation were only slightly modified, increased or decreased depend of the series of catalysts. The enantioselectivity obtained were moderate and close to the results for homogeneous catalysts, differently from the results obtained with less bulky ligands prepared by us before, this facts could be originated because these two series of ligands are too big for accommodating into mesopores. For improving the performance, reactivity and selectivity, of heterogenised catalysts we are going to modulate the steric volume of substrates and ligands with the different size of mesopores or channels in the zeolite.

4. Conclusions

The new rhodium-complexes are active for the hydrogenation of olefins. The heterogenisation on silica and USY-zeolite (containing supermicropores and a large quantity of silanol groups) increases the original activity remarkably for small olefins and the activity is maintained for dehydrophenylalanine derivatives. In hydrogenation reactions catalysed by the zeolite-heterogenised complexes the geometrical constraints have a strong impact on the reaction rates. Studies with another zeolite which presents a different structure and pore size are in progress. The heterogenised complexes are significantly more stable than their corresponding homogeneous complexes over prolonged reaction times and in the presence of traces of oxygen in the feedstock.

The high activities observed with these supported complexes, plus the fact that a prolonged activity can be achieved in continuous operation without detectable loss of rhodium from the support (as measured by atomic absorption), indicates that these are truly heterogeneous counterparts of homogeneous transition metal complex catalysts.

5. Supplementary material

Full details of the synthesis and characterisation of the ligands may be obtained from the authors.

Acknowledgements

The authors thank the Financial support from Dirección General de Investigación Científica y Técnica of Spain (Project MAT-94-0359-C02-02).

References

- [1] R. Selke, K. Häuptke, H.W. Krause, *J. Mol. Catal.*, 56 (1989) 315, and references therein.
- [2] C.U. Pittman, Jr., in: P. Hodge, D.C. Sherrington (Eds.), *Polymer Supported Reactions in Organic Synthesis*, Wiley, New York, 1980, p. 249-291.
- [3] F.R. Hartley, *Supported Metal Complexes*, D. Reidel, Dordrecht, 1985.
- [4] U. Nagel, E. Kinzel; *J. Chem. Soc. Chem. Comm.*, (1986) 1089.
- [5] N. Takashi, *J. Am. Chem. Soc.* 100 (1978) 264.
- [6] N. Ishizuka, M. Togashi, M. Inoue, S. Enomoto, *Chem. Pharm. Bull.* 35 (1987) 1686.
- [7] U. Nagel, *Angew. Chem. Int. Ed. Eng.* 23 (1984) 435.
- [8] A. Corma, M. Iglesias, C. del Pino, F. Sánchez, *J. Organomet. Chem.* 431 (1992) 233.
- [9] A. Corma, A. Carmona, M. Iglesias, A. San José, F. Sánchez, *J. Organomet. Chem.* 492 (1995) 11.
- [10] J. Chatt, L. Venanzi, *J. Chem. Soc.*, (1957) 4715.
- [11] D. Drew, J.R. Doyle, *Inorg. Synth.* 13 (1972) 48.
- [12] G. Giordano, R.H. Crabtree, *Inorg. Synth.* 28 (1990) 88.
- [13] J. A. Osborn, F. H. Jardine, J. F. Young, G. Wilkinson, *J. Chem. Soc. A*, (1966) 171.
- [14] J.A. Osborn, G. Wilkinson, *Inorg. Synth.* 28 (1990) 77.
- [15] A. Corma, A. Carmona, M. Iglesias, F. Sánchez, *Inorganica Chim. Acta.* 244 (1996) 239.
- [16] G. Szalintai, P. Sandor, J. Bakos, *Magn. Res. Chem.* 29 (1991) 449.
- [17] F.W. Wehrli, T. Wirthlin, *Interpretation of Carbon 13 NMR Spectra*, Heydel, London, 1978.
- [18] A. Adepapo, S.A. Benyunes, P.A. Chaloner, C. Claver, P.B. Hitchcock, A. Ruiz, N.A. Ruiz, *J. Organomet. Chem.* 443 (1993) 241.
- [19] L. Fidalgo, M.A. Garralda, R. Hernández, L. Ibarlucea, *J. Organomet. Chem.* 447 (1993) 299.
- [20] L.L. Murrell, in: J.J. Burton, R.L. Garten (Eds.), *Advanced Materials in Catalysis*, ch. 8, Academic Press, NY, 1977.
- [21] P.K. Iler, *The Chemistry of Silica*, Wiley, New York, 1979.
- [22] Tai-Nang Huang, J. Schwartz, *J. Am. Chem. Soc.* 104 (1982) 5244.
- [23] F. Mauge, A. Auroux, J. Courcelle, P. Engelhard, P. Gallezot, J. Grosmanin, in: B. Imelik, C. Naccache, G. Coudurier, Y. Ben Taarit, J.C. Védrine (Eds.), *Catalysis by Acids and Bases*, Elsevier Science B.V., Amsterdam, 1985, p. 99.